Türkiye Peyzaj Araştırmaları Dergisi
2023, 6:1, 56-74
Araştırma Makalesi

Turkish Journal of Landscape Research
2023, 6:1, 56-74
Research Article

EVALUATION OF THE RELATIONSHIP BETWEEN SPATIAL-TEMPORAL CHANGES OF LAND USE/LAND COVER (LULC) AND LAND SURFACE TEMPERATURE (LST): A CASE STUDY OF NİLÜFER, BURSA

Tuğba ÜSTÜN TOPAL[1*]

[1*] *Department of Landscape Architecture, Faculty of Fine Arts, Design and Architecture, Tekirdağ Namık Kemal University, 59030, Tekirdağ, Türkiye, tugbaustun61@gmail.com, ORCID: 0000-0002-9687-927X*

Abstract

This study was carried out in Nilüfer district of Bursa in order to reveal the extent of urbanization, to monitor the changes in landscape elements such as water, vegetation and agricultural lands, and to examine the effects of this on Land Surface Temperature (LST). For this purpose, images taken by Sentinel-2 satellites in 2017 and 2022 were used. With these images, NDVI (Normalized Difference Vegetation Index), SAVI (Soil Adjusted Vegetation Index), mNDWI (Modified Normalized Difference Water Index) and NDBI (Normalized Difference Built-up Index), which are widely used in understanding terrain changes, were calculated. Time series analyzes were made between the relevant years The relationship between the changes in the field and the surface temperature was questioned by calculating the LST value with Landsat 8 OLI_TIRS images, and the relations between the indexes and the LST were evaluated by correlation analysis. The results show that NDVI, SAVI, and mNDWI are on a decreasing trend between 2017-2022, while NDBI is on an increasing trend. In other words, the results showed that the vegetation areas and water-covered surfaces decreased, while the built-up areas increased. It has been observed that the changes in Land Use/Land Cover (LULC) increase the LST in the west and south regions of the district.

Keywords: *NDVI, SAVI, mNDWI, NDBI, GEE, Bursa*

ARAZİ KULLANIMI/ARAZİ ÖRTÜSÜ (AKAÖ)'NÜN MEKANSAL-ZAMANSAL DEĞİŞİMLERİ İLE YER YÜZEY SICAKLIĞI (YYS) ARASINDAKİ İLİŞKİNİN DEĞERLENDİRİLMESİ: NİLÜFER, BURSA ÖRNEĞİ

Özet

Bursa'nın Nilüfer ilçesinde gerçekleştirilen bu çalışma, kentleşmenin boyutlarını ortaya koymak, su, vejetasyon, tarım arazileri gibi peyzaj öğelerinin değişimlerini izlemek, ve bunun Yer Yüzey Sıcaklığı (YYS) üzerindeki etkilerini incelemek amacıyla gerçekleştirilmiştir. Bunun için Google Earth Engine (GEE) ve Coğrafi Bilgi Sistemleri (CBS)'den yararlanılmıştır. Çalışmada Sentinel-2 uyduları tarafından çekilen 2017 ve 2022 yıllarındaki görüntüler kullanılmıştır. Bu görüntüler ile arazi değişimlerini anlamada yaygın olarak kullanılan spektral indekslerden NDVI (Normalize Edilmiş Fark Bitki Örtüsü İndeksi), SAVI (Toprakla Düzeltilmiş Bitki Örtüsü İndeksi), mNDWI (Modifiye Edilmiş Normalize Fark Su İndeksi) ve NDBI (Normalize Edilmiş Fark Yerleşim Alanı Indeksi) hesaplanmıştır. İlgili yıllar arası zaman serisi analizleri yapılmıştır. Arazideki değişimlerin yüzey sıcaklığı ile nasıl bir ilişkisi olduğu Landsat 8 OLI_TIRS görüntüleri ile YYS değeri hesaplanarak sorgulanmış ve indeksler ile YYS arasındaki ilişkiler korelasyon analizi ile değerlendirilmiştir. Sonuçlar 2017-2022 yılları arasında NDVI, SAVI ve mNDWI'nin azalma trendinde olduğunu göstermekte, buna karşılık NDBI'nin ise artma trendinde olduğunu göstermektedir. Yani sonuçlar, vejetasyon alanlarının ve su ile kaplı yüzeylerin azaldığını, yapılaşmış alanların ise arttığını göstermiştir. Arazi Kullanımı/Arazi Örtüsü (AKAÖ)'ndeki değişimlerin ilçenin batı ve güney bölgelerinde YYS'yi arttırdığı görülmüştür.

Anahtar Kelimeler: *NDVI, SAVI, mNDWI, NDBI, GEE, Bursa*

Received (Geliş tarihi): 20.08.2023, **Accepted** (Kabul tarihi): 29.08.2023 *Corresponding author (İletişim yazarı: tugbaustun61@gmail.com)
Citation (Atıf): Topal T. Ü., (2023). Evaluation of the relationship between spatial-temporal changes of land use/land cover (lulc) and land surface temperature (lst): a case study of Nilüfer, Bursa. Turkish Journal of Landscape Research, 6 (1), 56-74, **DOI:** https://doi.org/10.51552/peyad.1346845

1. INTRODUCTION

In the current period, our world is facing a big wave of urban growth. It is estimated that 66% of the world's population will live in urban areas by 2050 (United Nations, 2014). With the rapidly increasing population around the world, the need for new settlements arises, which causes a rapid land use / land cover (LULC) change (Alademomi et al., 2022). These changes and transformations bring serious environmental consequences. Some of these problems are the increase in greenhouse gas emissions, the decrease in agricultural lands, the emergence of air and water pollution, the decrease in biological diversity, the deterioration of ecological cycles, regional climate changes, the increase of impermeable surfaces and the increase of urban heat island effects and the transformation of cities into unhealthy areas in terms of thermal comfort (Korkut et al., 2016; Zheng et al., 2021; Alademomi et al., 2022). The main reasons for the formation of the heat island effect in cities are changes in urban landscape composition and patterns. With the increase in population in these areas, the decrease in green areas and water-covered areas causes the heat to intensify (Ranagalage et al., 2017). On the other hand, the increase in hard and reflective surfaces in cities and the increase in the use of impermeable materials such as concrete and asphalt affect the temperature of urban environments (Keerthi Naidu & Chundeli, 2023). With the increase of impermeable surfaces in cities, the surface albedo decreases, the thermal conductivity of the surface changes, and thus heat storage occurs on the surfaces. This causes the land surface temperature (LST) to increase in urban area (Shahfahad et al., 2020).

Understanding the dynamics of urbanization and learning about the spatial distribution of urban areas is of great importance in order to solve a number of long and short-term problems, some of which are listed above (Li & Chen, 2018). As a matter of fact, these changes in LULC cause irreversible effects on the environment. That's why it's important to be monitored regularly (Hussain et al., 2020). This is also important for environmental management and planning studies (Zhang et al., 2009; Saini, 2021). Understanding the factors related to the formation of urban heat islands and the relationships between them is important and necessary for the improvement of urban living conditions. Therefore, studies in this context draw attention as an important issue in the field of landscape planning (Tonyaloğlu, 2019). For this, mapping of urban lands is very useful for monitoring the growth of these areas (Shah et al., 2022). Geographical information systems (GIS) and remote sensing (RS) methods used in this direction are the basic tools used for temporal and spatial monitoring of urban dimensions and density with LULC mapping and thus investigating the ecological effects of urbanization (Majeed et al., 2021). Since the 1960s, with the development of remote sensing (RS) technology and the ability to obtain high resolution satellite images, it has become common to measure LST. In recent years, these operations can be done with a series of technical formulas with the help of remotely sensed images (He et al., 2010; Liu & Zhang, 2011; Halder et al., 2021).

RS can provide basic data for mapping. However, the increase in image resolutions increases the data size, requiring more hardware costs for the user, and may cause the processes to take longer in terms of time. In particular, accessing and analyzing very large time series data sets is time-consuming and costly (Tassi & Vizzari, 2020). In the last decade, cloud-based platforms have become popular with the latest technological developments, allowing users to instantly access huge amounts of data and analyze it with high-performance computing resources without the need for downloading. Google Earth Engine (GEE) is a free platform that works with scripting via JavaScript and Python using web-based interfaces (Tassi & Vizzari, 2020; Floreano & de Moraes, 2021; Loukika et al., 2021).

There are many studies on the effects of LULC changes on the LST (Sun et al., 2012; Ranagalage et al., 2017). In this direction, a series of index-based indicators has been developed to demonstrate the LULC (Shah et al., 2022). Of these, the Normalized Difference Vegetation Index (NDVI) is used to evaluate vegetation, and the Normalized Difference Built-Up Index (NDBI) is used to evaluate established terrains. These indices are widely used to understand the spatio-temporal changes of LULC (Chen et al., 2006; Ranagalage et al., 2017; Jamei et al., 2019; Hussain et al., 2020). Soil-Adjusted Vegetation Index (SAVI), an index that emerged to improve NDVI, provides more sensitive and accurate results in terms of detecting less dense vegetation areas in cities with dense urban texture (Akyürek, 2020). Since water areas also differ in terms of thermal properties, Modified Normalized Difference Water Index (mNDWI), a water index, can be used to distinguish between water areas and non-water areas (Chen & Zhang, 2017).

Nilüfer district of Bursa has been facing a rapid population growth in recent years. On the other hand, it is seen that new settlements are built rapidly in the district. The aim of this study is to investigate the situation in the

land use/cover pattern and the effects of urban surface temperature in the Nilüfer district, which has experienced a remarkable population increase in recent years. In the study, high resolution Sentinel-2 remote sensing images of different time periods were analyzed with GEE, and NDVI, SAVI, mNDWI and NDBI indices were used to extract LULC information. Then, the surface temperature obtained from the thermal infrared band with Landsat 8 was analyzed. With this research, the following was obtained: (1) The changes in the LULC change over the 2017-2022 period were examined with the help of spectral indices, (2) Urban surface temperature variation has been observed for the period 2017–2022, (3) The relationship between LULC change and LST between these years in Nilüfer district was investigated, (4) In order to monitor and evaluate the urban thermal environment, the density of LULC and LST and how it changes over time and the relationships between them were examined by statistical analysis.

2. METARIAL AND METHOD

2.1. Study Area

Nilüfer district of Bursa was chosen as the study area (Figure 1). Bursa is located in the southeast of the Sea of Marmara, between 40 degrees longitude and 28-30 degrees latitude circles. It is 155 meters above sea level. The climate in the province, which generally has a temperate climate, also varies according to the regions. A mild and warm climate is encountered in the north, while a harsh climate is encountered in the south. The total area of the province is 10.819 km^2 (Anonymous, 2023). The largest water asset in the Nilüfer disrict is a part of Uluabat Lake.

Nilüfer district is one of the three central districts of Bursa with the status of Metropolitan Municipality. The area of the district is 50.776 ha. The boundaries of the municipality consist of 13 neighborhoods in 1987, the year of establishment of the municipality. In 2014, with the law numbered 6360, the number of neighborhoods increased to 64 after the villages were given the status of neighborhoods (Nilüfer Municipality, 2023a) (Figure 1).

Bursa province is one of the crowded cities of Türkiye. Population growth in the province shows an increasing trend in recent years. The population of Nilüfer district, which was 56.131 together with the villages in 1987, reached 536.365 in 2022 (TUIK, 2023; Nilüfer Municipality, 2023a). Considering the population data after 2010, it was seen that the biggest change was experienced in Nilüfer with an increase of +79.4% between the years 2010-2022. According to the total population change of Bursa between the same years, it is seen that Nilüfer district constitutes 40.2% of the population (TUİK, 2023) The population data of Nilüfer district between 2010-2022 are given in Figure 2.

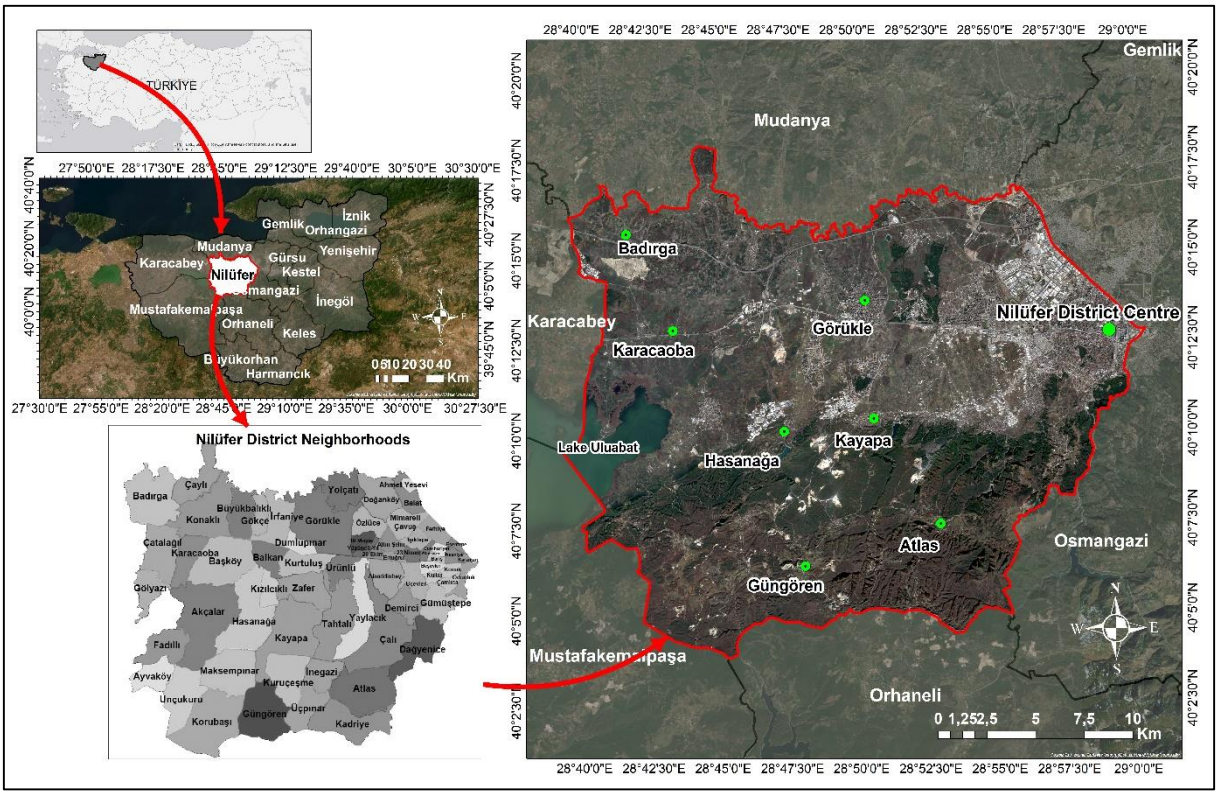

Figure 1. Study area (on the right Sentinel-2 satellite image dated 09.01.2023, B4,B3,B2 natural band combinations) (Prepared using Copernicus Open Access Hub, 2023 and Nilüfer Municipality, 2023b)

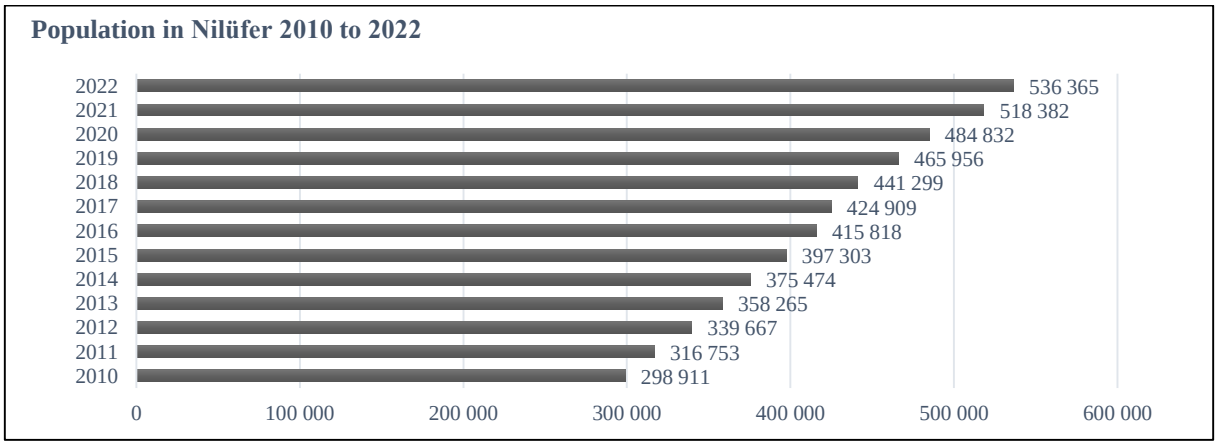

Figure 2. Population data of Nilüfer district between 2010-2022 (TUİK, 2023).

2.2. Google Earth Engine (GEE)

Remote sensing (RS) systems have been collecting large volumes of data sets for many years using some software and resources. However, the size of these data, their high spatio-temporal resolution and complexity can complicate their acquisition, processing, management and analysis (Amani et al., 2020; Yang et al., 2022). In this context, the revolutionary Google Earth Engine (GEE) developed by Google (Wang et al., 2020) was released in 2010 as a high-performance cloud computing platform with significant computational capabilities developed to provide solutions to these challenges (Gorelick et al., 2017; Hay Chung et al., 2021; Zhao et al., 2021). Thanks to GEE, it is easier to work with petabyte-scale geographical data over large areas (Mutanga & Kumar, 2019; Amani et al., 2020; Ashok et al., 2021). GEE provides scientific analysis and visualization of datasets (Xiong et al., 2017). On the other hand, GEE supports more geospatial data types, provides advanced algorithms to users for free with a web application. For these reasons, the interest in GEE, where analyzes can be made on a global scale, is increasing and its use has become increasingly widespread recently (Tamiminia et al., 2020; Wang et al., 2020; Zhao et al., 2021). GEE is used in a wide variety of analyzes by a wide variety

of professional groups. Global forest change, global surface water change, crop yield estimation, LULC classifications, urban mapping, flood mapping, fire mapping can be done with GEE (Hay Chung et al., 2021). Figure 3 shows the sample query screen for the maps produced in GEE for this study.

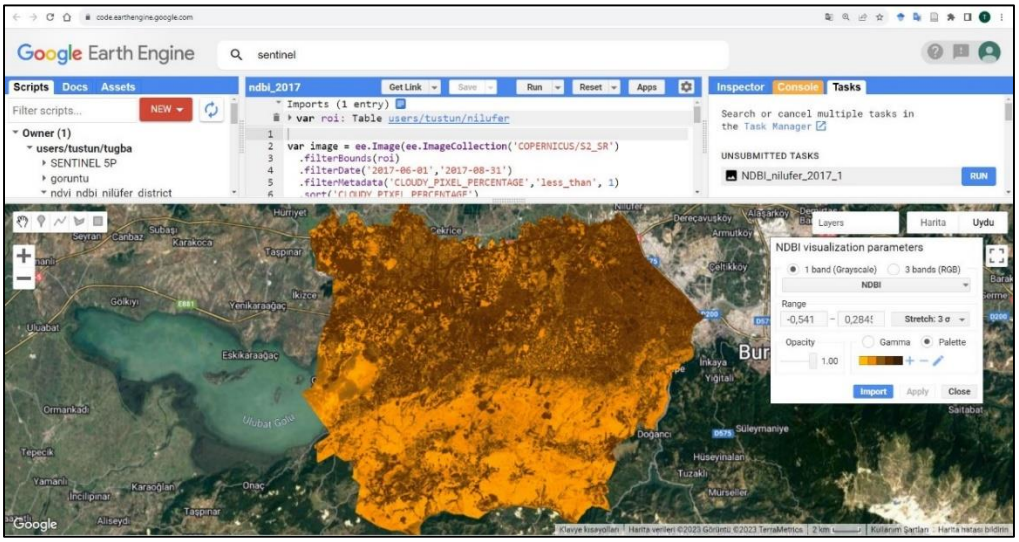

Figure 3. Example query screen for maps produced in GEE for this study

2.3. Data and Method

Boundary data for the study area covering Nilüfer district was downloaded from www.openstreetmap.org. (OpenStreetMap, 2023). Sentinel-2 MSI: MultiSpectral Instrument and Landsat 8 OLI_TIRS data were used in the study. Sentinel-2 images are dated 12/07/2017 and 28/07/2022. Sentinel-2 data was obtained from the GEE platform. After the analysis of the spectral indices of the relevant years and the time series graphics were made in the GEE environment, the map production was carried out with the help of the ArcMap 10.8 program. Sentinel-2 is a high-resolution, wide-area and multi-spectrum satellite that supports Copernicus field observation studies and provides monitoring of vegetation, soil and water cover as well as inland waterways and coastal areas (GEE, 2023). In the study, Landsat 8 images of the relevant years were used to make land surface temperature calculations. Landsat images are among the most widely used satellite images for LST calculations. In the selection of these images, it was paid attention to the images of the same month in order to reveal consistent analyzes, and images dated 09/07/2017 and 23/07/2022 were selected, respectively. The cloudiness of the images used in the study is less than 1%. Landsat 8 images were downloaded free of charge from the US Geological Survey's (USGS) website (USGS, 2023).

2.4. Calculation of Spectral Indices

In the study, 4 different indices and their time series between the years 2017-2022 were calculated. These are NDVI, SAVI, mNDWI and NDBI. These indices are spectral indices that are frequently used in land use and change analysis.

2.4.1. NDVI

The Normalized Difference Vegetation Index (NDVI) is one of the commonly used indices for mapping vegetation on a global scale (Zha et al., 2010). It was developed by Rouse et al (1973). NDVI uses spectral reflectance values obtained in the near-infrared and red part of the electromagnetic spectrum, respectively. The calculated value ranges from -1 to +1. NDVI values from -1 to 0 indicate no vegetation, while values close to +1 indicate the highest green vegetation density (Ekumah et al., 2020). According to the literature reviews, values below 0 represent water, snow, cloud. Values between 0 and 0.2 represent barren land /built up/rock. Values between 0.2 and 0.5 refer to the soil and vegetation mixture. Values above 0.5 represent areas covered with vegetation (Avdan & Jovanovska, 2016; Alex et al., 2017). The NDVI formula is given in the following equation (Rouse et al., 1973; Tucker & Sellers, 1986):

NDVI = (NIR - Red) / (NIR + Red)……eq (1).

2.4.2. SAVI

The Soil-Adjusted Vegetation Index (SAVI) is an index developed by Huete (1988) to improve NDVI. In areas where the vegetation cover is less than 40% and the soil surface is exposed, the reflection of the light in the red and near infrared spectrum affects the plant index values. This appears to be a problem when comparisons are made between soil types with different luminosity values that reflect different amounts of light in the red and near infrared wavelengths. Especially in cities with dense urban texture, SAVI gives more sensitive and accurate results than NDVI in terms of detecting vegetation areas with less density. Thus, SAVI is formulated in a similar way to NDVI and the difference from NDVI is that the soil brightness correction factor (L) is added (Sarp & Erener, 2017; Akyürek, 2020; Rhyma et al., 2020). The SAVI formula is given in the following equation:

SAVI = ((NIR - Red) / (NIR + Red + L)) * (1 + L)……eq (2).

The L value varies according to the amount and spread of green vegetation. It takes the value “0” in areas with very dense vegetation and “1” in areas where there is no green vegetation. Generally, L=0.5 is the default value used and works well in most cases (Sarp & Erener, 2017).

2.4.3. mNDWI

The Modified Normalized Difference Water Index (mNDWI) is a water index developed by Xu (2006). Since residential areas and open water areas are represented with positive values in the NDWI, this may cause confusion in discrimination, especially in regions with highly built-up areas. This new index was obtained by replacing the NIR band with the short wave infrared 1 (SWIR1) band in this index. Previous studies have shown that this index gives better results in detecting water areas (Singh et al., 2015). The mNDWI formula is given in the following equation:

mNDWI = (Green-SWIR1) / (Green + SWIR1) ……eq (3).

2.4.4. NDBI

In the literature, there are various spectral indices for the detection of residential areas using satellite images. Among them, the Normalized Difference Built-Up Index (NDBI), developed by Zha et al. (2010) (Bouhennache et al., 2018), is one of the indices with high accuracy and used in many studies (Kaimaris & Patias, 2016; Bramhe et al., 2018; Zuhairi et al., 2020). The NDBI uses the NIR and SWIR1 portions of the electromagnetic spectrum to distinguish built-up areas (Estoque & Murayama, 2015). The NDBI value ranges from -1 to +1. It is understood that the presence of built-up areas increases as it gets closer to +1. (Shahfahad et al., 2020). The NDBI formula is given in the following equation:

NDBI = (SWIR1 - NIR) / (SWIR1 + NIR)……eq (4).

In Table 1, the spectral indices used for the detection of LULC in this study and their equations for Sentinel 2 are given.

Table 1. Spectral indices used for the detection of LULC in this study and their equations for Sentinel-2

LULC indexes	Equation for Sentinel-2	References
NDVI (Normalized Difference Vegetation Index)	NDVI = (B08 – B04) / (B08 + B04)	(Rouse et al., 1973)
SAVI (Soil-Adjusted Vegetation Index)	SAVI = (B08 - B04) / (B08 + B04 + L) * (1.0 + L) L = 0.5	(Huete, 1988)

mNDWI (Modified Normalized Difference Water Index)	mNDWI= (B11- B3) / (B11 + B3)	(Xu, 2006)
NDBI (Normalized Difference Built-Up İndex)	NDBI = (B11 - B8) / (B11 + B8)	(Zha et al., 2010)

2.5. Calculation of Land Surface Temperature (LST)

Spectral radiance value transformation is applied to the thermal image band values (DN: Digital Number) that will be used to determine the land surface temperature, with the help of the parameters in the metadata file of the satellite image. In this equation, L λ represents the temperature of atmospheric spectral radiance, M L represents the band-specific multiplicative rescaling factor from the metadata, Q cal represents the quantized and calibrated standard product pixel values (DN), and AL represents the radiance additive rescaling factor (from satellite metadata) (Kumari et al., 2018; Akyürek, 2020).

Lλ= ML* Qcal+ AL……eq (5).

After this conversion, the TIRS band data is converted from spectral brightness to brightness temperature (BT) using the thermal constants provided in the metadata file. Results in Celsius are obtained by adding absolute zero to the radiation temperature and revising it (Avdan & Jovanovska, 2016). The BT luminance temperature (ºC) in this equation calculated by is taking Lλ; Spectral radiation, K1: band specific thermal conversion constant 774.8853, K2: band specific thermal conversion constant 1321,0789 (Güneş et al., 2021).

$$BT = \frac{\mathrm{K2}}{ln(\frac{K1}{\mathrm{L\lambda}}+1)} - 273.15$$ ……eq (6).

After this step, the Normalized Difference Vegetation Index (NDVI) must be calculated in order to determine the Earth's surface emissivity and vegetation ratio. In determining the LST, NDVI values should be obtained from reflectance values, not DN values. The NDVI value is calculated using the reflectance values of the near infrared and red bands. For Landsat 8 these are Band 5 and Band 4 respectively (Akyürek, 2020). (eq (1)).

After calculating the NDVI value, the proportion of the vegetation (Pv) is calculated using the equation below. Then, the land surface emissivity LSE (ε) value suggested by Sobrino et al.(2004) is calculated using the equation below (Kumari et al., 2018).

$Pv=((NDVI-NDVI_{MIN})/(NDVI_{MAX}-NDVI_{MIN}))^2$ ……eq (7).

ε=0.004Pv+0.986…….eq (8).

After calculating the LSE (ε) value, the last step is to calculate the LST value.

$$LST = \frac{\mathrm{BT}}{\{1+[(\lambda \mathrm{BT}/p)\ln\varepsilon\lambda]\}}$$ ……eq (9).

Here, wavelength λ=10.895 is used while calculating LST as Celsius (°C), and BT is at-sensor BT (°C) (Avdan & Jovanovska, 2016). The ρ value here is a fixed value and is calculated with the help of the formula given below:

ρ = h * c⁄s = 1.438 x 10-2 mK……..eq (10).

(h: Planck constant (6.626 * 10-34 Js), s: Boltzmann constant (1.38 * 10-23 J/K), c: Speed of light (2.998 * 108 m/s) (Akyürek, 2020).

3. FINDINGS AND DISCUSSION

3.1. Findings on Spectral Indices Results

When the NDVI analysis results are examined, it is seen that the maximum was calculated as 0,9992 for 2017 and 0,7259 for 2022. The mean value was calculated as 0,5190 for 2017 and 0,3427 for 2022. These results

are important in terms of showing that there has been a decrease in the areas covered with vegetation between 2017 and 2022 for the Nilüfer district. On the other hand, according to the classification made according to the NDVI results, the areas covered with water in 2017 were calculated as 1,966.86 ha. For the year 2022, the areas covered with water are calculated as 1,737.84 ha. These results show that there has been a decrease in the areas covered by water between the related years. According to the NDVI results, 6,647.66 ha of the study area was calculated as barren land/built up/rock for 2017, and this value was calculated as 11,969.96 ha in 2022. Soil and vegetation mixture areas were calculated as 15,010,94 ha for 2017, and 25,275.42 for 2022. The areas covered with vegetation were calculated as 28,784.41 ha for 2017 and 13,425.98 ha for 2022. According to these values, the NDVI results show that the areas covered with water and vegetation areas decreased, while the barren land/built up/rock areas increased between 2017-2022. (Figure 4).

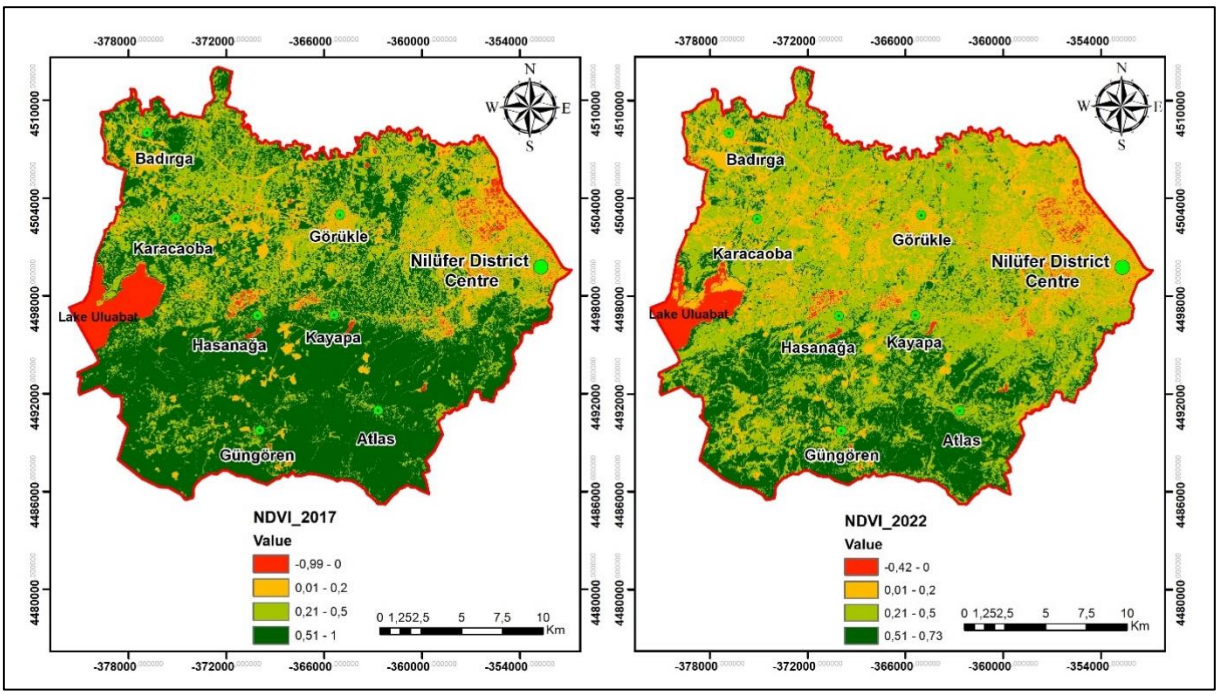

Figure 4. NDVI maps of 2017 and 2022 for Nilüfer district

According to the SAVI analysis results, it is seen that the values calculated for 2017 vary between 1,4986 and -1,4786 as maximum and minimum, respectively. The mean value calculated for 2017 was 0,7784. The values calculated for 2022 are maximum 1,0888 and minimum -0,6268. The mean value for the same year was 0,5139. According to the classification made according to the results of SAVI, the areas covered with dense vegetation were calculated as 33,497.25 ha for 2017 and 21,974.36 ha for 2022. When the SAVI maps of the relevant years are examined, it is clearly seen that the areas covered with dense vegetation have decreased in terms of area in 2022. (Figure 5). NDVI and SAVI results show parallelism in terms of revealing the decrease in vegetation areas.

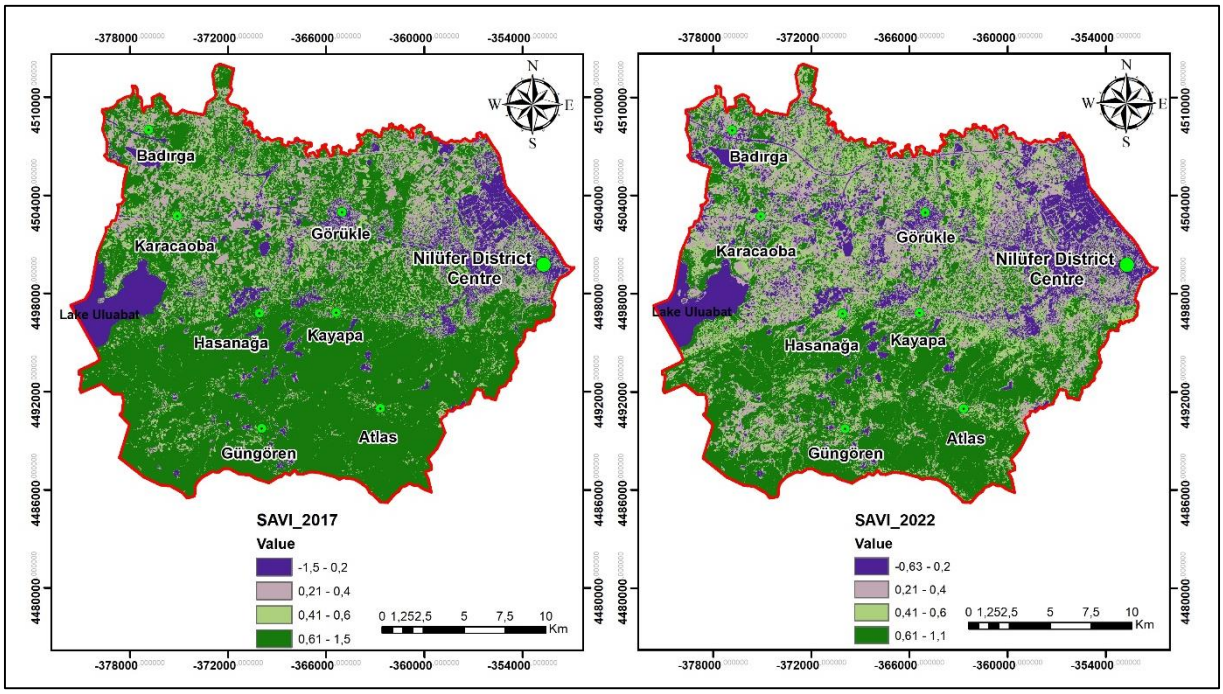

Figure 5. SAVI maps of 2017 and 2022 for Nilüfer district

According to the mNDWI analysis results, the maximum value calculated as 0,9998 for 2017 was calculated as 0,6643 for 2022. The minimum value for 2017 was calculated as -0,9029 and 0,6284 for 2022. The mean value was calculated as 0,4299 for 2017 and 0,2743 for 2022. When the areas covered with water are calculated in terms of area, while the areas covered with water were calculated as 1,758.81 ha in 2017, it was calculated as 1,730.08 ha for 2022. The largest water resource in the area is a part of Uluabat Lake. When the maps of the relevant years are examined, it is thought that the biggest reason for this change may be the shrinkage in this lake. (Figure 6). These results reveal that the areas covered with water in Nilüfer district shrank between 2017 and 2022 according to both NDVI results and mNDWI results. However, these results show parallelism with the results of previous studies carried out in Uluabat Lake. As a matter of fact, when the studies covering different time periods for the lake were examined, Aksoy & Ozsoy (2002), Tağıl (2004), Saçın (2010) and Topal & Baykal (2023) showed that the water surfaces decreased and the areas covered by the reeds and open soil surfaces increased in their studies. Although these results cover the whole lake, it is an important finding that this study, which was carried out in a part of the lake, also indicates the shrinkage in the lake.

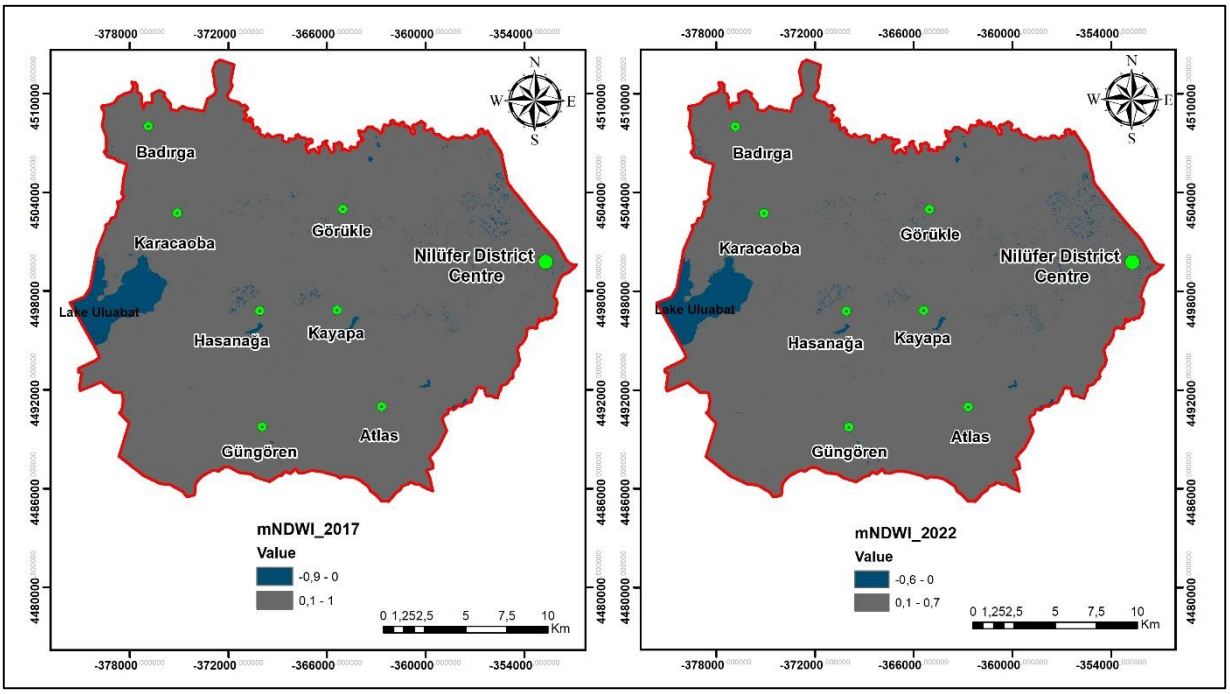

Figure 6. mNDWI maps of 2017 and 2022 for Nilüfer district

When the NDBI analysis results are examined, it is seen that the maximum value calculated as 0,9984 for 2017 is calculated as 0,5102 for the year 2022. The minimum value for 2017 was calculated as -0,7688, and for 2022 it was calculated as -0,6397. The mean value was calculated as -0,1300 for 2017 and -0,0831 for 2022. In order to understand the spatial distribution of the built-up areas, the maps were prepared by classifying the values. Accordingly, areas with values between -0.2 and -0.1 for 2017 cover 7,023.77 ha, and for 2022 these areas cover 10,550.98 ha. Areas with values between -0.1 and 0.4 for 2017 cover an area of 24,760.71 ha, and for 2022 these areas cover 29,855.61 ha. When Figure 7 is examined together with these results, it is seen that the newly built-up areas are spreading especially towards the west and south parts of the district.

Table 2 shows descriptive statistical data for the NDVI, SAVI, mNDWI and NDBI indices for the study area.

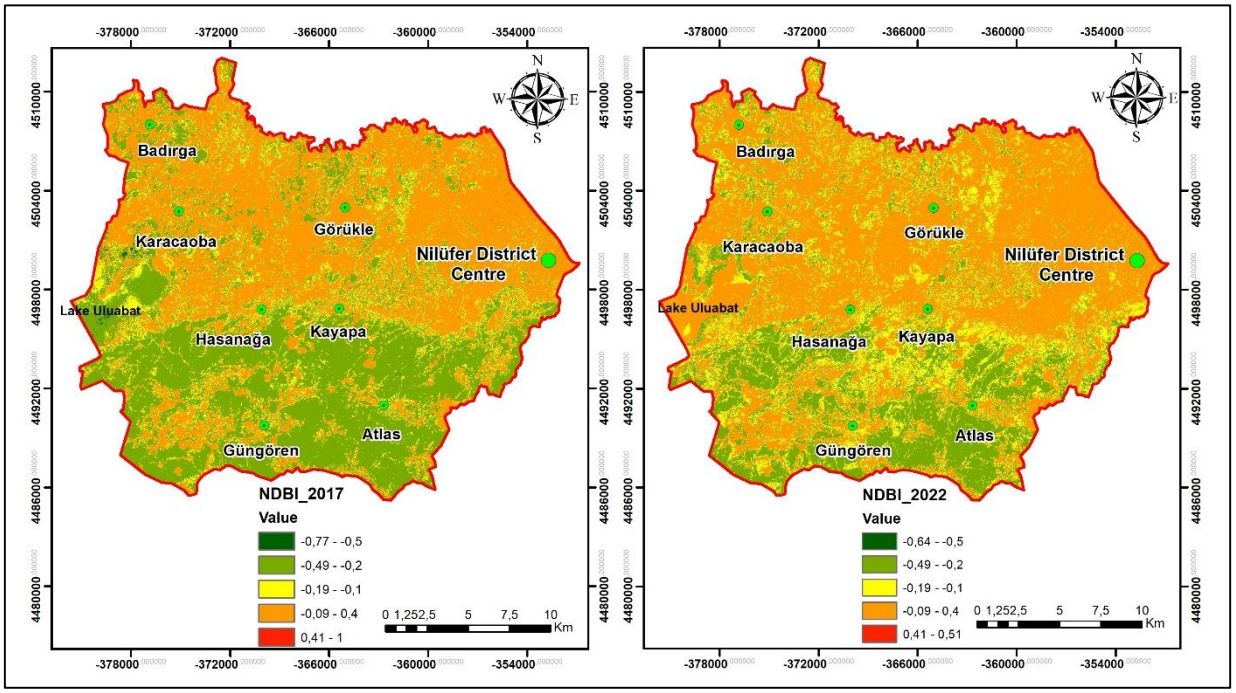

Figure 7. NDBI maps of 2017 and 2022 for Nilüfer district

Table 2. Descriptive statistical data for study area

Evaluation		Date	
		2017/07/12	**2022/07/28**
NDVI	Max	0,9992	0,7259
	Min	-0,9886	-0,4179
	Mean	0,5190	0,3427
	Stand. dev.	0,3038	0,1904
SAVI	Max	1,4986	1,0888
	Min	-1,4786	-0,6268
	Mean	0,7784	0,5139
	Stand. dev.	0,4556	0,2855
mNDWI	Max	0,9998	0,6643
	Min	-0,9029	-0,6284
	Mean	0,4299	0,2743
	Stand. dev.	0,2288	0,1085
NDBI	Max	0,9984	0,5102
	Min	-0,7688	-0,6397
	Mean	-0,1300	-0,0831
	Stand. dev.	0,1832	0,1290

In order to observe how the results of the NDVI, SAVI, mNDWI and NDBI indices, which took place from 2017 to 2022, have changed in the years between these dates and to observe this change trend, the situation between the relevant years has been graphed by performing time series analyzes on the GEE platform. When Figure 8 is examined, it is seen that NDVI, SAVI and mNDWI are in a decreasing trend for Nilüfer district between 2017-2022. It is clearly seen that NDBI is in an increasing trend. These results are important in terms of showing that vegetation areas decreased according to NDVI and SAVI calculations, water-covered areas decreased according to mNDWI calculations, and built areas increased according to NDBI calculations.

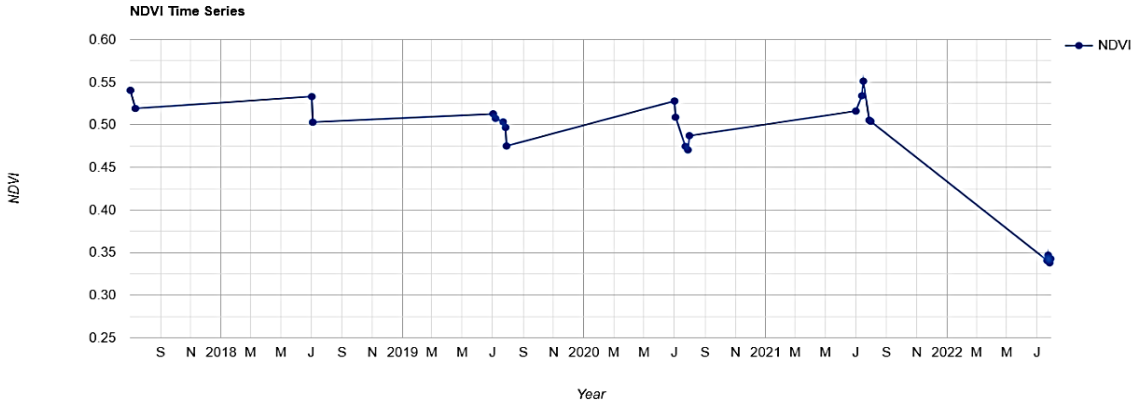
NDVI Time Series
NDVI
0.60
0.55
0.50
0.45
0.40
0.35
0.30
0.25
S N 2018 M M J S N 2019 M M J S N 2020 M M J S N 2021 M M J S N 2022 M M J
Year

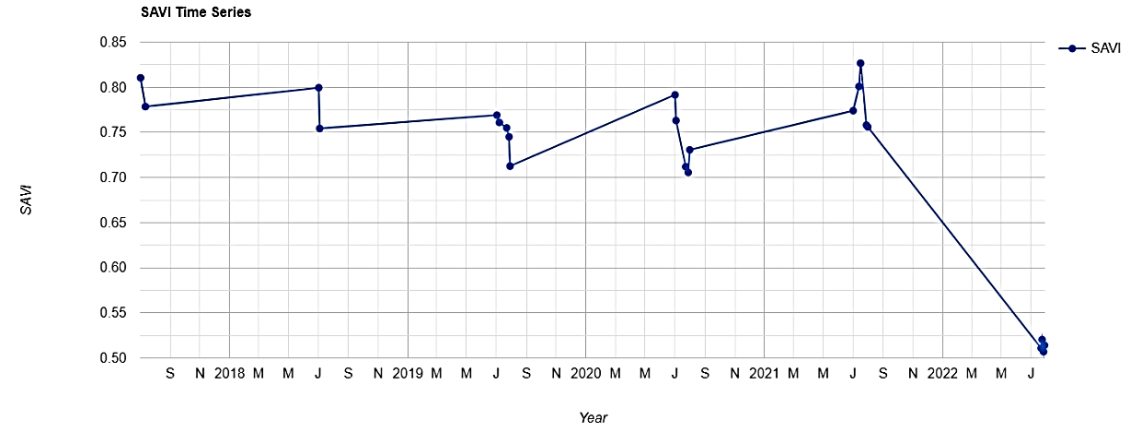
SAVI Time Series
SAVI
0.85
0.80
0.75
0.70
0.65
0.60
0.55
0.50
S N 2018 M M J S N 2019 M M J S N 2020 M M J S N 2021 M M J S N 2022 M M J
Year

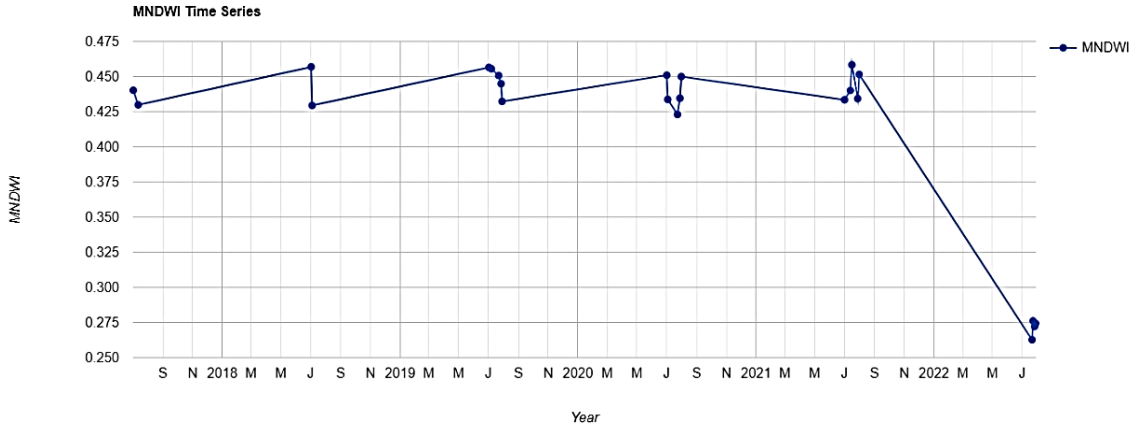
MNDWI Time Series
MNDWI
0.475
0.450
0.425
0.400
0.375
0.350
0.325
0.300
0.275
0.250
S N 2018 M M J S N 2019 M M J S N 2020 M M J S N 2021 M M J S N 2022 M M J
Year

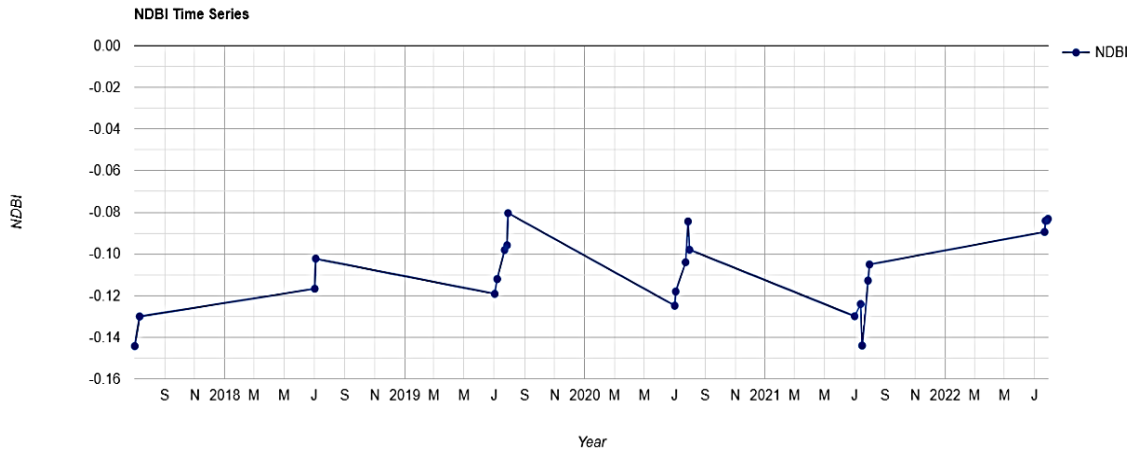
NDBI Time Series
NDBI
0.00
-0.02
-0.04
-0.06
-0.08
-0.10
-0.12
-0.14
-0.16
S N 2018 M M J S N 2019 M M J S N 2020 M M J S N 2021 M M J S N 2022 M M J
Year

Figure 8. Time series graphs produced in GEE for the NDVI, SAVI, mNDWI and NDBI indices of Nilüfer district for the years 2017-2022

3.2. Findings on Land Surface Temperature Calculations

By using Landsat 8 satellite images and applying the process steps described in land surface temperature calculations, land surface temperature maps of the study area for the years 2017 and 2022 were produced. (Figure 9). Land surface temperature values vary between 20.6 ºC and 50.1 ºC for 2017. The land surface temperature varies between 22.4 ºC and 49.4 ºC for 2022. According to these results, the maximum temperature difference in the area between 2017-2022 is 0.7 ºC and the minimum temperature difference is 1.8 ºC. The land surface temperature values were classified as 20.6ºC-25ºC, 25ºC-30ºC, 30ºC-35ºC, 35ºC-40ºC- and >40ºC and the areal distributions of the regions where these values were experienced were examined. According to the classification results, areas between 20.6°C-25°C were calculated as 10,601.57 ha for 2017, and areas between 22.4°C-25°C for 2022 were calculated as 3,176.35 ha. Areas between 25ºC-30ºC were calculated as 13,386.02 ha for 2017, and 14,715.78 ha for 2022. For 2017, the areas between 30ºC-35ºC were calculated as 20,428.68 ha, and for the year 2022, these areas were calculated as 22,928.40 ha. Areas between 35ºC-40ºC were calculated as 7,842.20 ha for 2017, and 11,513.96 ha for 2022. Areas with temperatures between 40 ºC - 50.1 ºC cover small areas and were calculated as 149.25 ha and 74.08 ha for 2017 and 2022, respectively. When these values and the maps given in Figure 9 are examined, it is seen that the land surface temperature, which varies between 20ºC-25ºC in the south parts of the district, has increased to values ranging between 25ºC-30ºC in 2022. It is seen that the parts where higher temperatures are observed spread towards the west parts of the district and the values in these regions vary between 30ºC-35ºC, increasing to values between 35ºC-40ºC by 2022.

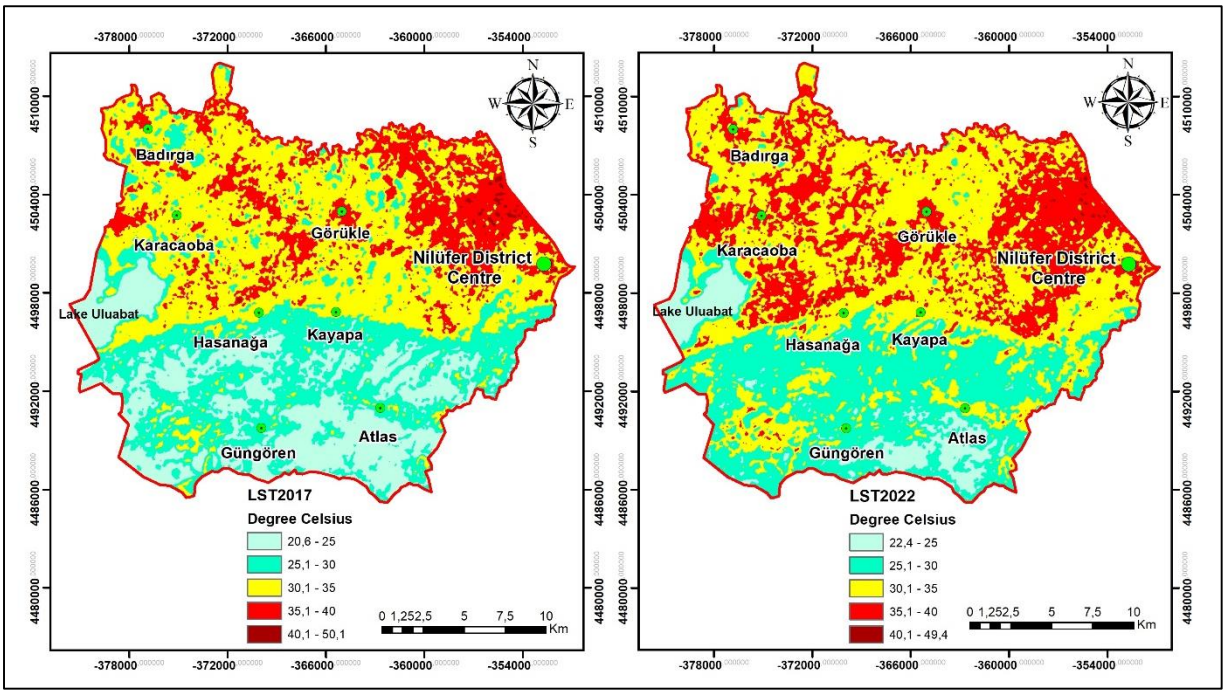

Figure 9. LST maps of 2017 and 2022 for Nilüfer district

3.3. The Relationship Between the NDVI, SAVI, mNDWI, NDBI and LST

Correlation analysis was performed to explain the relationship between the land surface temperature and the NDVI, SAVI, mNDWI and NDBI indices used to understand the land use change. In order to evaluate the results of 2017 and 2022, 396 points were randomly selected from the area and correlation analysis was performed. These relationships are seen in Figure 10. As a result, it was observed that NDBI values were high in regions with high land surface temperatures, and NDVI and SAVI values were higher in regions with low land surface temperatures. Correlation analysis results show that land surface temperature is negatively correlated with NDVI and SAVI, and positively correlated with NDBI. The correlation coefficient between LST and NDVI was calculated as r=-0,570099 for 2017 and r=-0,571664 for 2022. The correlation coefficient

between LST and SAVI was calculated as r=-0,570142 for 2017 and r=-0,571667 for 2022. The correlation coefficient between land surface temperature and NDBI was calculated as r=0,752465 for 2017 and r=0,685774 for 2022.

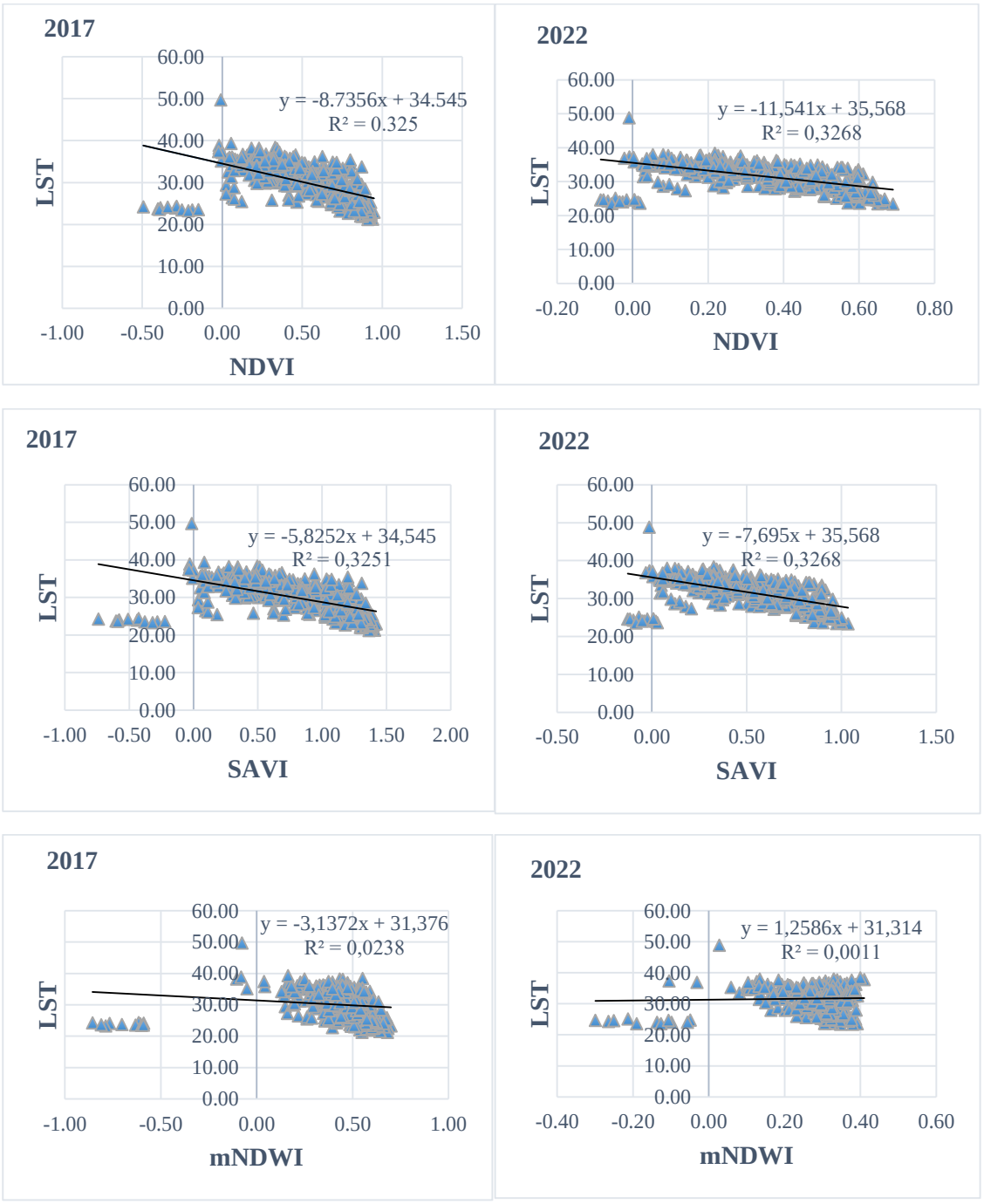

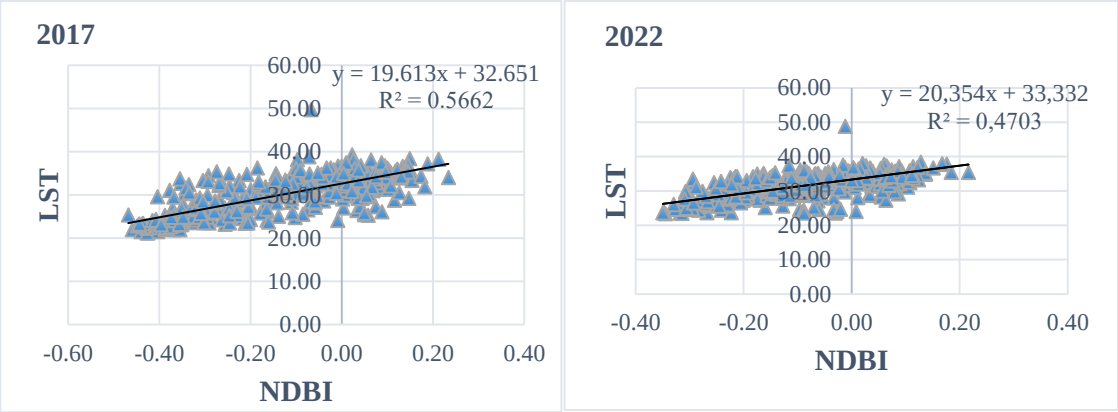

Figure 10. The relationship between the NDVI, SAVI, mNDWI, NDBI and LST

The results of the negative and positive relationships of NDVI and NDBI with LST are in parallel with many studies in the literature (Chen & Zhang, 2017; Ranagalage et al., 2017; Malik et al., 2019; Jamei et al., 2019; Shahfahad et al., 2020; Halder et al., 2021; Yamak et al., 2021; Alademomi et al., 2022; Değerli & Çetin, 2022). The negative relationship between SAVI and LST also supports the study results of Akyürek (2020).

4. CONCLUSION ADN EVALUATION

In this study, it was examined how LULC change affected LST in the period between 2017-2022 in Nilüfer district of Bursa. The relationships between the NDVI, SAVI, mNDWI and NDBI indices used for this and the LST were statistically questioned. Index calculations and time series graphs produced through the GEE platform show that NDVI, SAVI and mNDWI are in a decreasing trend, while NDBI is in an increasing trend.

In the study, LST maps prepared from Landsat 8 satellite image data represent the spatial distribution of land surface temperature in the district. In the study, it was observed that there was an inversely proportional relationship between NDVI, SAVI and LST. In other words, LST analysis results show higher surface temperature in built-up areas and bare surfaces, and lower surface temperatures in healthy vegetation areas. For this reason, while cities are growing, increasing green areas will decrease the land surface temperature. In other words, increasing the density and quantity of green areas in this direction, implementing applications such as green roofs and green walls in places where structural surfaces are dense, and carrying out road planting works on pedestrian paths and sidewalks will be effective. On the other hand, the reduction of impermeable surfaces is also an important factor for controlling the surface temperature. These measures that can be taken in cities are very important in terms of ensuring urban thermal comfort and public health.

Considering the spatial distribution of NDBI and LST results, it was seen that the built-up areas spread towards the west and south of Nilüfer district and it was an important finding that these areas gave high LST results. In other words, it has been observed that LST has a directly proportional relationship with NDBI. The correlation results of the study also showed that LST and NDBI were in a stronger relationship. Therefore, it is understood that NDBI has a greater effect on LST than other indices examined. In this way, it can be recommended to follow the NDBI results to understand the LST as well as in which areas urban heat island effects are effective. All these results are important in terms of showing how visible the LULC change and its land surface temperature effects are even in a short period of 2017-2022.

Nilüfer district is a center of attraction that receives high immigration and provides employment opportunities to a large part of Bursa's population. Factors such as the fact that 9 of the 18 Organized Industrial Zones (OIZs) in the province are located in Nilüfer (Nilüfer Municipality, 2023a), the existence of factories of many industrial enterprises, the presence of university and the presence of many private and public schools are effective in the emergence of this. However, this intense migration, as experienced in many cities that grew and became urbanized rapidly, caused the district to develop in a housing-oriented manner, and this caused the decrease of agricultural areas, the emergence of air and water pollution, the increase of waste, and the insufficiency of green areas. The findings of the study show that the expansion of the district center is in a direction towards Görükle, Zafer, Kayapa, Akçalar neighborhoods. In this context, it is thought that this study, which shows such rapid population growth and urban growth and deals with Nilüfer district, will be an

exemplary and useful study for other regions in terms of showing the results of land use/land cover change. In addition, it is thought that the results will be beneficial to local governments and the departments of the state that make city plans.

As a result, mapping and monitoring statistical results in monitoring urban growth provide important information for professional disciplines related to physical planning and policy makers. In the analysis of the results, the data is important as well as the choice of the methods used in the analysis of these data. As a matter of fact, it is very important and necessary for ensuring development in a way that gives the necessary importance to environmental factors and for sustainable development and sustainable urbanization. For this reason, it is thought that such studies, which provide numerical information about urban growth and environmental change, will be useful in policies and regulations for local and regional development.

REFERENCES

Aksoy, E., & Özsoy, G. (2002, June). Investigation of multi-temporal land use/cover and shoreline changes of the Uluabat Lake Ramsar Site using RS and GIS. In *Proceedings of the International Conference on Sustainable Land Use and Management*. 73-79.

Akyürek, Ö. (2020). Termal Uzaktan Algılama Görüntüleri İle Yüzey Sıcaklıklarının Belirlenmesi: Kocaeli Örneği. *Doğal Afetler ve Çevre Dergisi*, *6*(2), 377–390.

Alademomi, A. S., Okolie, C. J., Daramola, O. E., Akinnusi, S. A., Adediran, E., Olanrewaju, H. O., Alabi, A. O., Salami, T. J., & Odumosu, J. (2022). The interrelationship between LST, NDVI, NDBI, and land cover change in a section of Lagos metropolis, Nigeria. *Applied Geomatics*, *14*(2), 299–314.

Alex, E., Ramesh, K., & Hari, S. (2017). Quantification and understanding the observed changes in land cover patterns in Bangalore. *International Journal of Civil Engineering and Technology*, *8*, 597–603.

Amani, M., Ghorbanian, A., Ahmadi, S. A., Kakooei, M., Moghimi, A., Mirmazloumi, S. M., Moghaddam, S. H. A., Mahdavi, S., Ghahremanloo, M., Parsian, S., Wu, Q., & Brisco, B. (2020). Google Earth Engine Cloud Computing Platform for Remote Sensing Big Data Applications: A Comprehensive Review. *IEEE Journal of Selected Topics in Applied Earth Observations and Remote Sensing*, *13*, 5326–5350.

Anonymous. (2023). Nüfus, Konum, İklim ve Coğrafya https://www.bursa.com.tr/tr/sayfa/nufus-konum-iklim-ve-cografya-47/ Access date: 31.03.2023

Ashok, A., Rani, H. P., & Jayakumar, K. V. (2021). Monitoring of dynamic wetland changes using NDVI and NDWI based landsat imagery. *Remote Sensing Applications: Society and Environment*, *23*, 100547.

Avdan, U., & Jovanovska, G. (2016). Algorithm for Automated Mapping of Land Surface Temperature Using LANDSAT 8 Satellite Data. *Journal of Sensors*, 1-8. e1480307.

Bouhennache, R., Bouden, T., Taleb-Ahmed, A., & Cheddad, A. (2018). A new spectral index for the extraction of built-up land features from Landsat 8 satellite imagery. *34*(14), 1531–1551.

Bramhe, V. S., Ghosh, S. K., & Garg, P. K. (2018). Extraction of Built-Up Area By Combining Textural Features and Spectral Indices From Landsat-8 Multispectral Image. *The International Archives of the Photogrammetry, Remote Sensing and Spatial Information Sciences*, *XLII–5*, 727–733.

Chen, X., & Zhang, Y. (2017). Impacts of urban surface characteristics on spatiotemporal pattern of land surface temperature in Kunming of China. *Sustainable Cities and Society*, *32*, 87–99.

Chen, X.L., Zhao, H.M., Li, P.X., & Yin, Z.Y. (2006). Remote sensing image-based analysis of the relationship between urban heat island and land use/cover changes. *Remote Sensing of Environment*, *104*(2), 133–146.

Copernicus Open Access Hub. (2023). Sentinel-2 images. https://scihub.copernicus.eu/dhus/#/home Access date: 31.03.2023

Değerli, B., & Çetin, M. (2022). Evaluation from rural to urban scale for the effect of NDVI-NDBI indices on land surface temperature, in Samsun, Türkiye. *Turkish Journal of Agriculture-Food Science and Technology*, *10*(12), 2446-2452.

Ekumah, B., Armah, F. A., Afrifa, E. K. A., Aheto, D. W., Odoi, J. O., & Afitiri, A. R. (2020). Geospatial assessment of ecosystem health of coastal urban wetlands in Ghana. *Ocean & Coastal Management*, *193*. 105226.

Estoque, R. C., & Murayama, Y. (2015). Classification and change detection of built-up lands from Landsat-7 ETM+ and Landsat-8 OLI/TIRS imageries: A comparative assessment of various spectral indices. *Ecological Indicators*, *56*, 205–217.

Floreano, I. X., & de Moraes, L. A. F. (2021). Land use/land cover (LULC) analysis (2009–2019) with Google Earth Engine and 2030 prediction using Markov-CA in the Rondônia State, Brazil. *Environmental Monitoring and Assessment*, *193*(4), 239.

Gorelick, N., Hancher, M., Dixon, M., Ilyushchenko, S., Thau, D., & Moore, R. (2017). Google Earth Engine: Planetary-scale geospatial analysis for everyone. *Remote Sensing of Environment*, *202*, 18–27.

Google Earth Engine (GEE). (2023). https://code.earthengine.google.com/ Sentinel-2 MSI: MultiSpectral Instrument. Access date: 30.03.2023

Güneş, C., Pekkan, E., & Tün, M. (2021). Eskişehir Kent Merkezinde Yer Alan Üniversite Kampüslerindeki Kentsel Isı Adası Etkilerinin LANDSAT-8 Uydu Görüntüleri Üzerinden Araştırılması. *Ulusal Çevre Bilimleri Araştırma Dergisi*, *4*(1), 22–32.

Halder, B., Bandyopadhyay, J., & Banik, P. (2021). Monitoring the effect of urban development on urban heat island based on remote sensing and geo-spatial approach in Kolkata and adjacent areas, India. *Sustainable Cities and Society*, *74*, 103186.

Hay Chung, L. C., Xie, J., & Ren, C. (2021). Improved machine-learning mapping of local climate zones in metropolitan areas using composite Earth observation data in Google Earth Engine. *Building and Environment*, *199*, 107879.

He, C., Shi, P., Xie, D., & Zhao, Y. (2010). Improving the normalized difference built-up index to map urban built-up areas using a semiautomatic segmentation approach. *Remote Sensing Letters*, *1*(4), 213–221.

Huete, A. R. (1988). A soil-adjusted vegetation index (SAVI). *Remote Sensing of Environment*, *25*(3), 295–309.

Hussain, S., Mubeen, M., Ahmad, A., Akram, W., Hammad, H. M., Ali, M., Masood, N., Amin, A., Farid, H. U., Sultana, S. R., Fahad, S., Wang, D., & Nasim, W. (2020). Using GIS tools to detect the land use/land cover changes during forty years in Lodhran District of Pakistan. *Environmental Science and Pollution Research*, *27*(32), 39676–39692.

Jamei, Y., Rajagopalan, P., & Sun, Q. (Chayn). (2019). Spatial structure of surface urban heat island and its relationship with vegetation and built-up areas in Melbourne, Australia. *Science of The Total Environment*, *659*, 1335–1351.

Kaimaris, D., & Patias, P. (2016). Identification and Area Measurement of the Built-up Area with the Built-up Index (BUI). *International Journal of Advanced Remote Sensing and GIS*, *5*(1), 1844–1858.

Keerthi Naidu, B. N., & Chundeli, F. A. (2023). Assessing LULC changes and LST through NDVI and NDBI spatial indicators: A case of Bengaluru, India. *GeoJournal*, *88*(4), 4335–4350.

Korkut, A., Gültürk, P., & Üstün Topal, T. (2016). Kentsel Peyzaj Yapılarında Zemin Geçirimliliği Üzerine Bir Araştırma: Tekirdağ Örneği. *Kastamonu Üniversitesi Orman Fakültesi Dergisi*, *16*(2), 412-422.

Kumari, B., Tayyab, M., Shahfahad, Salman, Mallick, J., Khan, M. F., & Rahman, A. (2018). Satellite-Driven Land Surface Temperature (LST) Using Landsat 5, 7 (TM/ETM+ SLC) and Landsat 8 (OLI/TIRS) Data and Its Association with Built-Up and Green Cover Over Urban Delhi, India. *Remote Sensing in Earth Systems Sciences*, *1*(3), 63–78.

Li, K., & Chen, Y. (2018). A Genetic Algorithm-Based Urban Cluster Automatic Threshold Method by Combining VIIRS DNB, NDVI, and NDBI to Monitor Urbanization. *Remote Sensing*, *10*(2), 277.

Liu, L., & Zhang, Y. (2011). Urban Heat Island Analysis Using the Landsat TM Data and ASTER Data: A Case Study in Hong Kong. *Remote Sensing*, *3*(7), 1535-1552.

Loukika, K. N., Keesara, V. R., & Sridhar, V. (2021). Analysis of Land Use and Land Cover Using Machine Learning Algorithms on Google Earth Engine for Munneru River Basin, India. *Sustainability*, *13*(24), 13758.

Majeed, M., Tariq, A., Anwar, M. M., Khan, A. M., Arshad, F., Mumtaz, F., Farhan, M., Zhang, L., Zafar, A., Aziz, M., Abbasi, S., Rahman, G., Hussain, S., Waheed, M., Fatima, K., & Shaukat, S. (2021). Monitoring of Land Use–Land Cover Change and Potential Causal Factors of Climate Change in Jhelum District, Punjab, Pakistan, through GIS and Multi-Temporal Satellite Data. *Land*, *10*(10), 1026.

Malik, M. S., Shukla, J. P., & Mishra, S. (2019). Relationship of LST, NDBI and NDVI using landsat-8 data in Kandaihimmat watershed, Hoshangabad, India. *Indian Journal of Geo Marine Sciences*, 48 (01), 25-31.

Mutanga, O., & Kumar, L. (2019). Google Earth Engine Applications. *Remote Sensing*, *11*(5), 591.

Nilüfer Municipality. (2023a). 2022-2024 Strategic Plan. https://www.nilufer.bel.tr/i/pdf/83.pdf, Access date: 26.08.2023.

Nilüfer Municipality. (2023b). Nilüfer Municipality new neighborhood boundaries. https://www.nilufer.bel.tr/ Access date: 26.08.2023

OpenStreetMap (2023). Available online: https://www.openstreetmap.org/, Access date: 26.08.2023

Ranagalage, M., Estoque, R. C., & Murayama, Y. (2017). An Urban Heat Island Study of the Colombo Metropolitan Area, Sri Lanka, Based on Landsat Data (1997–2017). *ISPRS International Journal of Geo-Information*, *6*(7), 189.

Rhyma, P. P., Norizah, K., Hamdan, O., Faridah-Hanum, I., & Zulfa, A. W. (2020). Integration of normalised different vegetation index and Soil-Adjusted Vegetation Index for mangrove vegetation delineation. *Remote Sensing Applications: Society and Environment*, *17*, 100280.

Rouse, Jr. J. W., Haas, R. H., Schell, J. A., & Deering, W., D. (1973). *Monitoring the vernal advancement and retrogradation (green wave effect) of natural vegetation*. (No. E75-10354).

Saçın Y. (2010). *Investigation of The Kocacay Delta and Uluabat Lake By Using Remote Sensing Methods.* Master's thesis, Balıkesir University, Institute of Science, Department of Civil Engineering, Balıkesir, Turkey.

Saini, V. (2021). Mapping Environmental Impacts of Rapid Urbanisation and Deriving Relationship between NDVI, NDBI and Surface Temperature: A Case Study. *IOP Conference Series: Earth and Environmental Science*, *940*(1), 012005.

Sarp, G., & Erener, A. (2017). Barajların Çevresel Etkilerinin Zamansal ve Mekansal Olarak Uzaktan Algılama İle Değerlendirilmesi: Atatürk Barajı Örneği. *Geomatik Dergisi Journal of Geomatics*, *2*(1), 1–11.

Shah, S. A., Kiran, M., Nazir, A., & Ashrafani, S. H. (2022). Exploring NDVI and NDBI Relationship Using Landsat 8 OLI/TIRS in Khangarh Taluka, Ghotki. *Malaysian Journal of Geosciences*, *6*(1), 08–11.

Shahfahad, Kumari, B., Tayyab, M., Ahmed, I. A., Baig, M. R. I., Khan, M. F., & Rahman, A. (2020). Longitudinal study of land surface temperature (LST) using mono- and split-window algorithms and its relationship with NDVI and NDBI over selected metro cities of India. *Arabian Journal of Geosciences*, *13*(19), 1040.

Singh, K. V., Setia, R., Sahoo, S., Prasad, A., & Pateriya, B. (2015). Evaluation of NDWI and MNDWI for assessment of waterlogging by integrating digital elevation model and groundwater level. *Geocarto International*, *30*(6), 650–661.

Sun, Q., Wu, Z., & Tan, J. (2012). The relationship between land surface temperature and land use/land cover in Guangzhou, China. *Environmental Earth Sciences*, *65*(6), 1687–1694.

Tağıl, Ş. (2004, September). Landuse & Landcover Change of Uluabat Wetland Using Remore Sensing and GIS. In *Turkey 9th ESRI and ERDAS Users Group Meeting*, 21-22.

Tamiminia, H., Salehi, B., Mahdianpari, M., Quackenbush, L., Adeli, S., & Brisco, B. (2020). Google Earth Engine for geo-big data applications: A meta-analysis and systematic review. *ISPRS Journal of Photogrammetry and Remote Sensing*, *164*, 152–170.

Tassi, A., & Vizzari, M. (2020). Object-Oriented LULC Classification in Google Earth Engine Combining SNIC, GLCM, and Machine Learning Algorithms. *Remote Sensing*, *12*(22), Article 22.

Tonyaloğlu, E. E. (2019). Kentleşmenin kentsel termal çevre üzerindeki etkisinin değerlendirilmesi, efeler ve İncirliova (Aydın) örneği. *Türkiye Peyzaj Araştırmaları Dergisi*, *2*(1), 1-13.

Topal, T. U., & Baykal, T.M. (2023). Monitoring the changes of Lake Uluabat Ramsar site and its surroundings in the 1985-2021 period using RS and GIS methods. *Global Nest Journal*, *25*(3), 103-114.

Tucker, C. J., & Sellers, P. J. (1986). Satellite remote sensing of primary production. *International Journal of Remote Sensing*, *7*(11), 1395–1416.

Türkiye İstatistik Kurumu (TÜİK). (2023). İstatistik Göstergeler. İl Göstergeleri, Toplam Nüfus. 2017 yılı İl ve İlçe Nüfusları. https://biruni.tuik.gov.tr/ilgosterge/?locale=tr Access date: 04.04.2023.

United Nations. (2014). *World urbanization prospects: The 2014 revision, highlights. Department of Economic and Social Affairs.*

United States Geological Survey (USGS). (2023). EarthExplorer – Home. https://earthexplorer.usgs.gov/ Access date: 31.03.2023

Wang, L., Diao, C., Xian, G., Yin, D., Lu, Y., Zou, S., & Erickson, T. A. (2020). A summary of the special issue on remote sensing of land change science with Google earth engine. *Remote Sensing of Environment*, *248*, 112002.

Xiong, J., Thenkabail, P. S., Gumma, M. K., Teluguntla, P., Poehnelt, J., Congalton, R. G., Yadav, K., & Thau, D. (2017). Automated cropland mapping of continental Africa using Google Earth Engine cloud computing. *ISPRS Journal of Photogrammetry and Remote Sensing*, *126*, 225–244.

Xu, H. (2006). Modification of normalised difference water index (NDWI) to enhance open water features in remotely sensed imagery. *International Journal of Remote Sensing*, *27*(14), 3025–3033.

Yamak, B., Yağci, Z., Bilgilioğlu, B. B., & Çömert, R. (2021). Investigation of the effect of urbanization on land surface temperature example of Bursa. *International Journal of Engineering and Geosciences*, *6*(1), 1-8.

Yang, L., Driscol, J., Sarigai, S., Wu, Q., Chen, H., & Lippitt, C. D. (2022). Google Earth Engine and Artificial Intelligence (AI): A Comprehensive Review. *Remote Sensing 2022*, *Vol. 14*, *Page 3253*, *14*(14), 3253.

Zha, Y., Gao, J., & Ni, S. (2010). Use of normalized difference built-up index in automatically mapping urban areas from TM imagery. *International journal of remote sensing*, 24(3), 583-594.

Zhang, Y., Odeh, I. O. A., & Han, C. (2009). Bi-temporal characterization of land surface temperature in relation to impervious surface area, NDVI and NDBI, using a sub-pixel image analysis. *International Journal of Applied Earth Observation and Geoinformation*, *11*(4), 256–264.

Zhao, Q., Yu, L., Li, X., Peng, D., Zhang, Y., & Gong, P. (2021). Progress and trends in the application of google earth and google earth engine. *Remote Sensing*, *13*(18), 3778.

Zheng, Y., Tang, L., & Wang, H. (2021). An improved approach for monitoring urban built-up areas by combining NPP-VIIRS nighttime light, NDVI, NDWI, and NDBI. *Journal of Cleaner Production*, *328*, 129488.

Zuhairi, A., Nur Syahira Azlyn, A., Nur Suhaila, M. R., & Mohd Zaini, M. (2020). Land Use Classification and Mapping Using Landsat Imagery for GIS Database in Langkawi Island. *Science Heritage Journal*, *4*(2), 59–63.